Life-based Geometric Design of HVDC Cables. Part 2: Effect of Electrical and Thermal Transients

Life-based Geometric Design of HVDC Cables. Part 2: Effect of Electrical and Thermal Transients

Bassel Diban, *Member, IEEE,* Giovanni Mazzanti, *Fellow, IEEE* and Paolo Seri, *Member, IEEE*

***Abstract*— This study, in two parts, investigates the design of HVDC cables depending on electrothermal life modelling of the insulating material. The first part investigated the way in which different parameters affect the design of an HVDC cable in steady state conditions, i.e. with known nominal voltage and ampacity. This paper investigates the effect of electrical (i.e. voltage) transients, such as voltage polarity reversals, in addition to thermal transients (such as load cycles of cable current) on the electrothermal life map of HVDC cables, and their influence on cable feasibility. An ad hoc MATLAB code has been developed for this study. Results show a considerable negative effect of electrical transients on the expected life. A more severe effect of electrical transiens is noticed for materials with a lower value of the temperature coefficient of conductivity, due to a longer duration of transients. On the contrary, thermal transients associated with load cycles – which mostly imply current values equal to or lower than cable ampacity – imply insulation temperature values always lower than the maximum permissible temperature, thus they have a positive effect on the electrothermal life, since the thermal stress applied on the cable insulation will be reduced, allowing for smaller cable geometries for a fixed voltage and ampacity rating. It must be noticed that only the electrothermal life is investigated in this paper, and other types of stresses (e.g. mechanical stress) may also affect insulation life, but this is out of the scope of this study.**

***Index Terms*— cable design, high voltage, HVDC transmission, life estimation, power cables, power system transients.**

I. INTRODUCTION

THE recent development in High Voltage Direct-Current cables technologies shows the continuous aim at manufacturing cables with greater voltage and/or ampacity [1,2]. For instance, many HVDC cable projects are being installed with rated voltage up to 600 kV [3,4]. Additionally, a higher voltage (640 kV) HVDC-XLPE cable system was also fully qualified in [5]. The latter implies the development of innovative HVDC cable insulations to be able to withstand both higher steady-state and transient voltages (up to rated voltage 800 kV) and/or temperatures, which is still a matter of research so far [6,7]. Since higher voltage necessarily means greater and more severe electrical transients, the effect of Temporary OverVoltages (TOVs) and Super-imposed Switching Impulses (SSI) on the reliability of HVDC extruded cables has been investigated in the most recent studies found in the literature [8,9], while other studies investigated the effect of polarity reversal on HVDC cables [10]. Design of HVDC cables in addition to the importance of the insulating materials development were highlighted in [7]. Part 1 of this paper investigated the effect of several parameters on the life of HVDC cables in steady state conditions, i.e. with known nominal voltage and ampacity, by means of a parametric study of an electrothermal life model on different cable geometries [11]. While this paper (part 2), investigates the effect of both electrical transients and thermal transients on the electrothermal life map of HVDC cables and their effect on the cable geometries. In this study, voltage polarity reversal (VPR) events are chosen to be studied as electrical transients, due to their severe effect on polymeric HVDC cables whereby the electric field significantly increases within a relatively long period of time. The full explanation of the concepts bringing to a life map and its 5 boundary constraints can be found in [11], and will only be quickly reviewed at the end of section II of this paper.

II. THEORETICAL BACKGROUND

A. Steady-state Electric Field

In this study, the DC electric field is calculated by means of the analytical closed-form formula introduced by Eoll in [12].

$$E_{DC}(r) = U_0 \frac{\delta}{r_o \cdot [1 - (r_i/r_o)^{\delta}]} (r/r_o)^{\delta-1} \qquad (1)$$

where r_i, r_o are the inner and outer insulation radii, respectively. r is a generic radius. δ is the field inversion coefficient which can be calculated as follows [1]:

$$\delta = \frac{\frac{aW_c}{2\pi\lambda_{T,d}} + bE_m}{1 + bE_m} = \frac{\frac{a\Delta T_d}{\ln(r_o/r_i)} + \frac{bU_0}{r_o - r_i}}{1 + bU_0/(r_o - r_i)} \qquad (2)$$

ΔT_d is the temperature drop between the inner insulation, r_i, and the outer insulation, r_o, in K. E_m is the mean value of the electric field (in kV/mm). $\lambda_{T,d}$ is the thermal conductivity of the dielectric (in W/(m K)). a and b are the temperature and field coefficients of the electrical conductivity σ, which is given by the following empirical expression [13]:

The authors are with the Department of Electrical, Electronic and Information Engineering (DEI), Alma Mater Studiorum–University of Bologna, 40136 Bologna, Italy (e-mail: bassel.diban2@unibo.it).

Color versions of one or more of the figures in this article are available online at http://ieeexplore.ieee.org

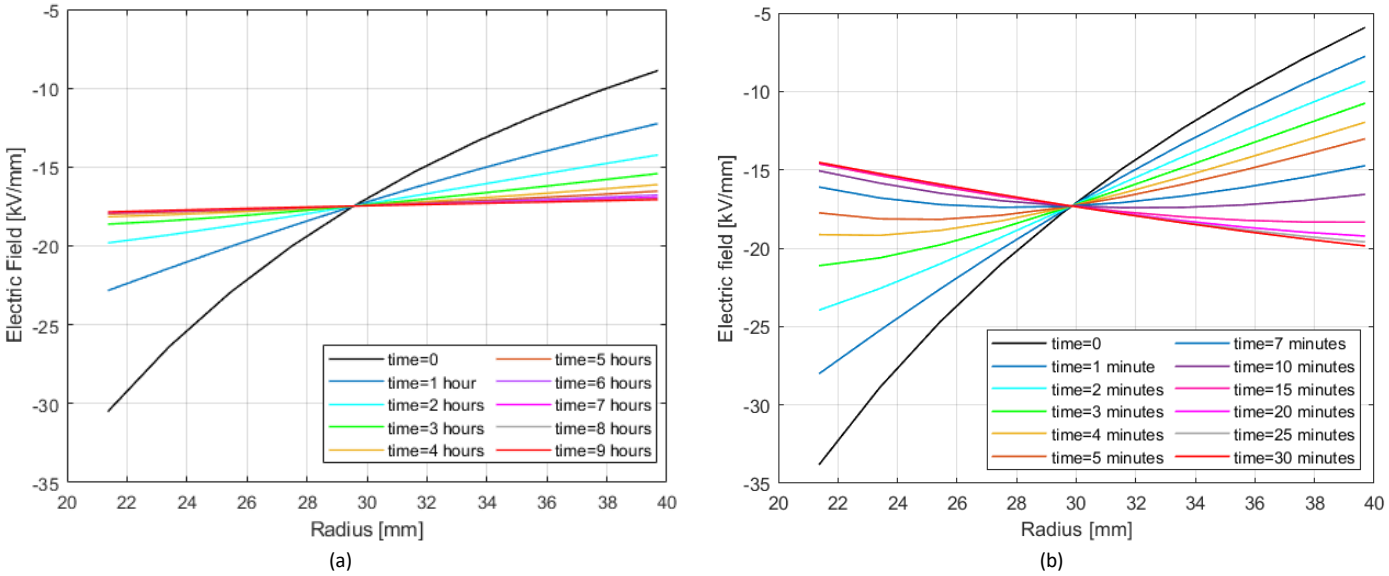

Fig. 1. Electric field variation over the period $5\tau_E$ during the second electrical transient after a VPR from $+U_0 \rightarrow -U_0$ for the so-called reference cable in hot conditions and (a) $a = 0.042$ and (b) $a = 0.084$. The main design data of the reference cable are listed in bold in Table I.

$$\sigma(r,t) = \sigma_0 \, exp(aT(r,t) + bE(r,t)) \qquad (3)$$

where σ_0 is the value of σ at 0 °C and for an electric field equal to 0 kV/mm.

B. Electrical Transients

In this paper, voltage polarity reversal (VPR) is studied as an electrical transient due to its severe effect on HVDC polymeric cables. Generally speaking, VPRs in HVDC systems can be of two types, namely:

1) **Fast VPRs**, whereby the absolute value of voltage falls to 0 and then rises to the opposite polarity in some hundred ms, with no relaxation. Fast VPRs take place during perturbations to respond promptly to adverse events;
2) **Slow VPRs**, whereby the absolute value of voltage falls to 0 in a few hundred ms, followed by some minutes of relaxation time, then it rises to the opposite polarity in a few hundred ms. Slow VPRs occur in normal operation to follow the needs of the electrical energy market.

As such, VPRs can be divided into 2 parts [10]:

1) a first transient referred hereafter to as tr_1, occurring while the polarity of the applied voltage is reversed (i.e. $+U_0 \rightarrow -U_0$ or $-U_0 \rightarrow +U_0$). This transient lasts hundreds of milliseconds in fast VPRs, while it lasts a few minutes in normal operation;
2) a second transient, referred hereafter to as tr_2, is the field transient occurring after the VPR, when the voltage applied is opposite to the voltage before the VPR.

This study investigates only fast VPRs. As such:

i) during the first electrical transient the field distribution within the cable switches from the initial resistive to a subsequent quasi-capacitive distribution;
ii) during the second electrical transient the charges inside the insulation thickness redistribute within a period ranging between minutes to hours, until the electric field reaches a resistive distribution. For the sake of simplicity and computational efficiency, the electric field variation during such second electrical transient is represented here according to the following approximated exponential model, previously introduced in [10], [14], and validated in [15] giving uncertainty lower than 2% for fast VPR, see Fig. 1:

$$E(r,t) = E_2(r) + [E_1(r) - E_2(r)] \cdot exp(-t/\tau_E(E,T)) \qquad (4)$$

where t is the generic time, $\tau_E(E,T)$ is the electrical time constant of the insulating material of the cable, which is given in DC systems by the following equation:

$$\tau_E(E,T) = \varepsilon/\sigma(E,T) \qquad (5)$$

$E_1(r)$, and $E_2(r)$ are the electric fields at the beginning of the second transient tr_2 and at the steady state after the VPR, respectively. The profiles within insulation thickness of $E_1(r)$ and $E_2(r)$ during the second electrical transient after a VPR from $+U_0$ to $-U_0$ for the so-called reference cable (the main design data of the reference cable are listed in bold in Table I) in hot conditions are represented in Fig. 1 by the black and red curves, respectively. Those fields are given by the following equations [16]:

Transient
$$E_1(r) = E_{DC} - 2E_{ac}(r) = E_{DC} - 2U_0/r \ln(r_o/r_i) \qquad (6)$$

Steady state
$$E_2(r) = -E_{DC} \qquad (7)$$

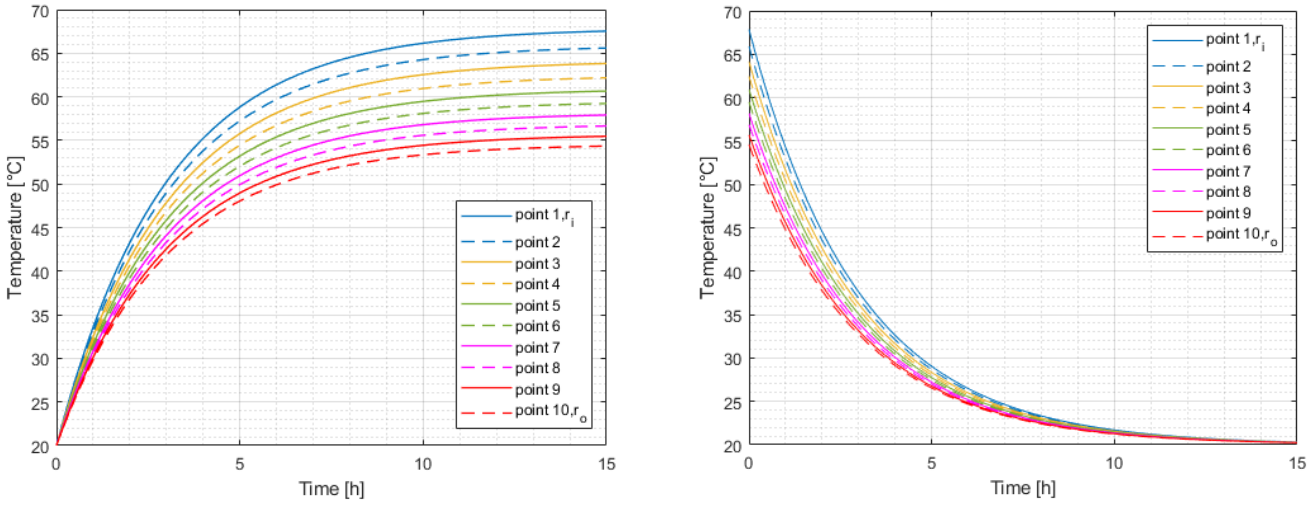

Fig. 2. Temperature transients over time = $5\tau_T$ at 10 evenly spaced points inside the insulation thickness (a) $LT \rightarrow HT$ transient and (b) $HT \rightarrow LT$ transient. The LT→HT transient and HT→LT transient are described in Table III.

Due to the negligible time duration of the first transient tr_1 in fast polarity reversal, only the second transient tr_2 will be investigated in this study. It is also worth noting that the time between two consecutive VPRs is assumed to be greater than or equal to $5\tau_E$ i.e., hence the steady state is supposed to be always reached after tr_2.

C. Thermal Transients

Thermal transients reflect the load cycles to which the cable is subjected throughout the year due to the load variation and in turn the variation in heat dissipation from the conductor across the insulation, see Fig. 2 (the LT→HT transient and HT→LT transient are described in Table III). Strictly speaking, the rigorous treatment of such thermal transients would require the use of high order "ladder-type" equivalent thermal models made of multiple cascaded series thermal resistances and shunt thermal capacitances, as prescribed by Standard IEC 60853 [17]. However - again for the sake of simplicity and computational efficiency - the thermal transients are also represented here according to the following approximated exponential model:

$$T(r,t) = T_2(r) + [T_1(r) - T_2(r)] \cdot exp(-t/\tau_T) \qquad (8)$$

where $T_1(r)$ is the initial temperature and $T_2(r)$ is the steady-state temperature. Equation (8) is the step response of a simplified first-order thermal circuit in which both the initial and the steady-state temperature is pre-defined to assure that the steady state temperature is reached and the load cycle is fully represented by the transient.

The validation of the approximated exponential transient thermal model vs. the higher order models recommended by IEC 60853 in [17] for MV and HV cables can be found in [18], [19], [20], [21], [14]. The temperature distribution within the insulation thickness $T(r)$ is found from considerations detailed in [17, 22], bringing to the following equation:

$$T(r) = T(r_i) - [T(r_i) - T(r_o)]\, ln\left(\frac{r}{r_i}\right) / ln\left(\frac{r_o}{r_i}\right) \qquad (9)$$

D. Life Model

Life estimation is based on the Inverse Power Model (IPM) and Arrhenius electro-thermal life models which can be expressed as follows [13], [23], [24]:

$$L(E,T) = L_D . [E/E_D]^{-n_D}\, exp(-B(1/T_D - 1/T)) \qquad (10)$$

where: $L(E,T)$ is life at a DC electric field E and temperature T (in K). E_D, T_D and L_D are design electric field, temperature and life respectively, n_D is the value of the voltage endurance coefficient (VEC) at temperature T_D, $B = \Delta W / k_B$, ΔW is the activation energy of the main thermal degradation reaction (in J), $k_B = 1.38 \times 10^{-23}\, J/K$ is the Boltzmann constant.

Considering a reference time t_{tot} (e.g. $t_{tot} = 1yr$), a steady state fraction, t_{ss}, can be defined as:

$$t_{ss} = t_{tot} - t_{tr} \qquad (11)$$

where t_{tr} is the cumulative duration of all transient periods occurring within the same reference time t_{tot}. Consequently, the loss of life occurring during the steady state period t_{ss} within the reference time t_{tot} can be written as follows, according to Miner's law of cumulated aging [25]:

$$LF_{ss}\big(E(r),T(r)\big) = \int_{t=0}^{t_{ss}} \frac{dt}{L_{ss}\big(E(r,t),T(r,t)\big)} = \frac{t_{ss}}{L_{ss}\big(E(r),T(r)\big)} \qquad (12)$$

where L_{ss} is life obtained from (10), and fields and temperatures are considered constants (since that is the case during t_{ss}). Accordingly, life loss during a single transient can be found by:

$$LF_{tr,i}\big(E(r),T(r)\big)=\int_{t=0}^{5\tau}\frac{dt}{L_{tr}\big(E_i(r,t),T_i(r,t)\big)} \quad (13)$$

where τ is the time constant, it is either the time constant of the electrical transient τ_E or the time constant of the thermal transient τ_T depending on the type of the transient. L_{tr} is life obtained from (10), and considering both the electrical and thermal fields, E_i, T_i are variables with time and the type of the transient i.e. electrical or thermal. The total loss of life occurring within t_{tot} can be attained by cumulating the loss of life during both the steady-state period LF_{ss} and a number n of transient events [8], [9], [25]:

$$LF\big(E(r),T(r)\big)=LF_{ss}\big(E(r),T(r)\big)+\sum_{i=1}^{n}LF_{tr,i}\big(E(r),T(r)\big) \quad (14)$$

Then, life (e.g in years) of insulation at different points in the cable insulation thickness can be estimated as follows:

$$L\big(E(r),T(r)\big)=t_{tot}/LF\big(E(r),T(r)\big) \quad (15)$$

Then, cable life is defined by the shortest life found within the insulation thickness:

$$L=\min_{r_i\le r\le r_o}\Big(L\big(E(r),T(r)\big)\Big) \quad (16)$$

Finally, life map is plotted in (r_i, r_o) coordinates and defined by limits given by 5 constrained quantities, i.e.:

1) maximum dielectric temperature $T_{max}=70\,°C$
2) maximum temperature drop across the insulation, $\Delta T_{max}=20\,°C$
3) maximum electric field $E_{max}=40\,kV/mm$
4) minimum conductor current density $J_{min}=0.6\,A/mm^2$
5) maximum extrusion radius $r_{o,max}=80\,mm$.

In the life map, the colored area includes all feasible designs of the cable, while the white area represents the infeasible designs due to violation of one (or more) of the above-mentioned constraints. Colors in the life map represents the relevant equi-life loci, as shown in Fig. 4 and 8 [11].

III. Case Study

Table I presents the main design parameters of the HVDC cable. The bold numbers are the values of a reference cable design, with inner and outer insulation radii set to $(r_i, r_o) = (21.4, 39.7)$ mm, whose design life is 40 years. In particular, the bold values of a and b are typical values for DC-XLPE insulation, according to scientific literature [26].

Table II shows the parameters of the electrical transients considered in this study. The initial electric field is the electric field directly after fast polarity reversal whereas the steady-state field is the resistive DC electric field distribution. It is worth

TABLE I
MAIN DESIGN PARAMETERS OF THE HVDC CABLE

Cable parameters	Symbol and unit		value
Design life	L_D [years]		**40**
Voltage Endurance Coefficient n_D	[a.u.]		**10**
Design temperature	T_D [°C]		**55**
Design electric field	E_D [kV/mm]		**20**
Rated voltage	U_0 [kV]		**320**
Maximum conductor temperature	T_{max} [°C]		**70**
Temperature coefficient of conductivity	a [1/°C]	a_L	0.042
		a_M	**0.084**
Stress coefficient of conductivity	b [mm/kV]		**0.03**
Thermal resistivity of dielectric	$\rho_{T,d}$ [K.m/W]		**3.5**
Thermal resistivity of sheath	$\rho_{T,sh}$ [K.m/W]		**3.5**
Thermal resistivity of soil	$\rho_{T,so}$ [K.m/W]		**1.3**

TABLE II
PARAMETERS AND CHARACTERISTICS OF ELECTRICAL TRANSIENTS

Parameter	symbol		Value
State 1	E_1		E distribution directly after polarity reversal (6)
State 2	E_2		Resistive electric field distribution (7)
Direction			$tr2$: $E_1 \rightarrow E_2$, tr_1 is neglected
Transient equation			(4)
Electrical time constant	τ_E		(5)
Transients frequency	n_E	a_L	0
			1 per month
			1 per week
			2 per week
			1 per day
			2 per day
		a_M	0
			1 per month
			1 per week
			2 per week
			1 per day
			2 per day
			5 per day
			10 per day

TABLE III
PARAMETERS AND CHARACTERISTICS OF THERMAL TRANSIENTS

Parameter	Symbol and unit	Value
State 1 of $T_{conductor}$	T_1 [°C]	Ambient temperature 20
State 2 of $T_{conductor}$	T_2 [°C]	Full load temperature
Direction		$T_1 \rightarrow T_2$
		$T_2 \rightarrow T_1$
Transient equation		(8)
Thermal time constant	τ_T [h]	1
		3
Transients frequency	n_T	0
		1 per day

noting that the time required to reverse the applied voltage is neglected here, being much shorter than the dielectric relaxation transient considered in Equation (4) (hundreds of milliseconds vs. minutes to hours). The electrical transients are applied during t_{tr}, while the resistive DC electric field is used for the calculations during t_{ss}. The number of electrical transients falls in the range from 1 transient per month up to 10 transients per day, as polarity reversals occur from few times per year to many per week according to [27] (it should also be pointed out that 10 events are an upper limit of transients within one single day, which occurs only on a minority of the overall service days of the cable system). However, this number is limited in this study to 2 electrical transients per day when considering low values of the temperature coefficient of conductivity, a, causing the increase of the time constant of the insulation, as shown in Fig. 3. A higher number of transients in this case would make the transients period longer than the total period $t_{tr} > t_{tot}$. Table III presents the parameters of the thermal transients. Two types of thermal transients are investigated i.e., heating transient ($T_1 \rightarrow T_2$) and cooling transient ($T_2 \rightarrow T_1$), applied on the cable during the transient period t_{tr}. A full load (hot cable) is used for steady-state calculations during t_{ss}. Thermal time constant τ_T ranges from 1 hour to many hours depending on the surrounding environment, burial depth …etc [28], [29]. In this study, two values of the thermal time constant are investigated i.e., 1 hour corresponding to air environment and 3 hours for soil environment. One transient per day is chosen for this study, i.e., one cycle includes both thermal transients ($T_1 \rightarrow T_2$ and $T_2 \rightarrow T_1$) every other day.

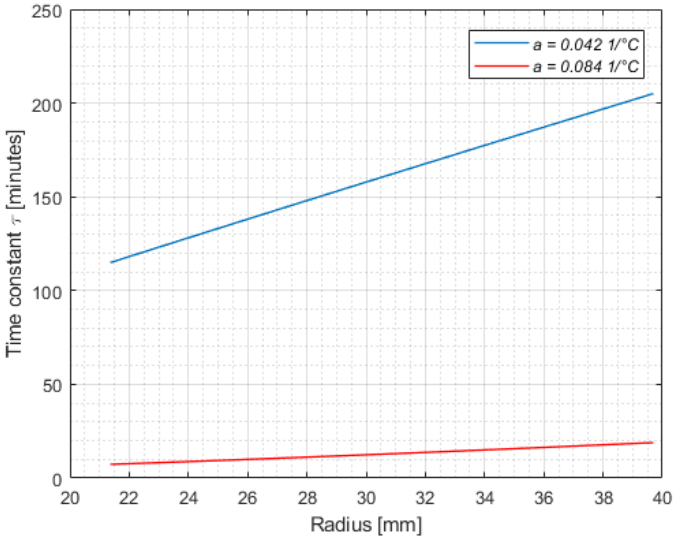

Fig. 3. Electrical time constant $\tau = \varepsilon/\sigma$ for a hot reference cable ($r_i = 21.4$, $r_o = 39.7$ mm), for $a = 0.042$ and $a = 0.084$.

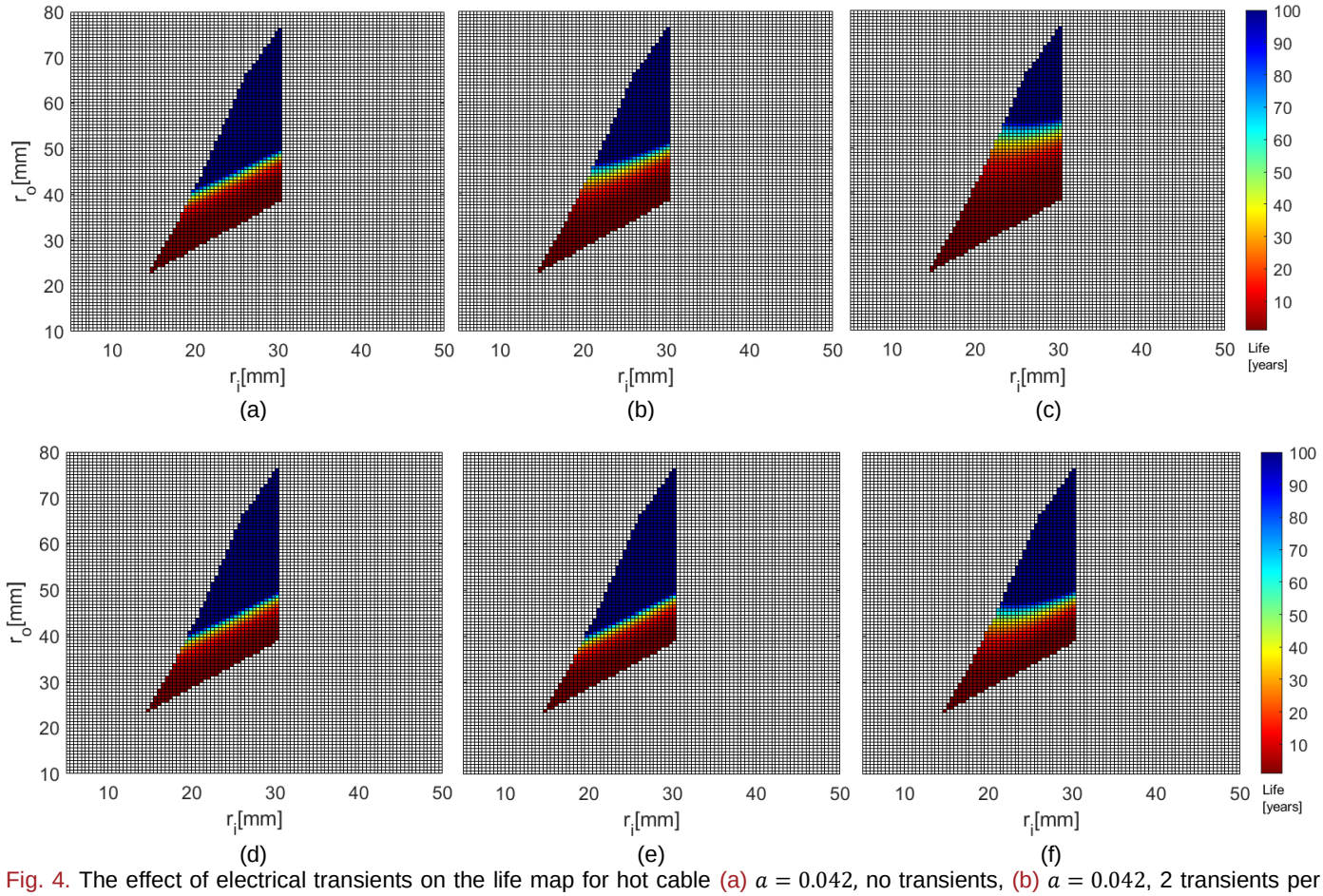

Fig. 4. The effect of electrical transients on the life map for hot cable (a) $a = 0.042$, no transients, (b) $a = 0.042$, 2 transients per week, (c) $a = 0.042$, 2 transients per day, (d) $a = 0.084$, no transients, (e) $a = 0.084$, 2 transients per week and (f) $a = 0.084$, 2 transients per day.

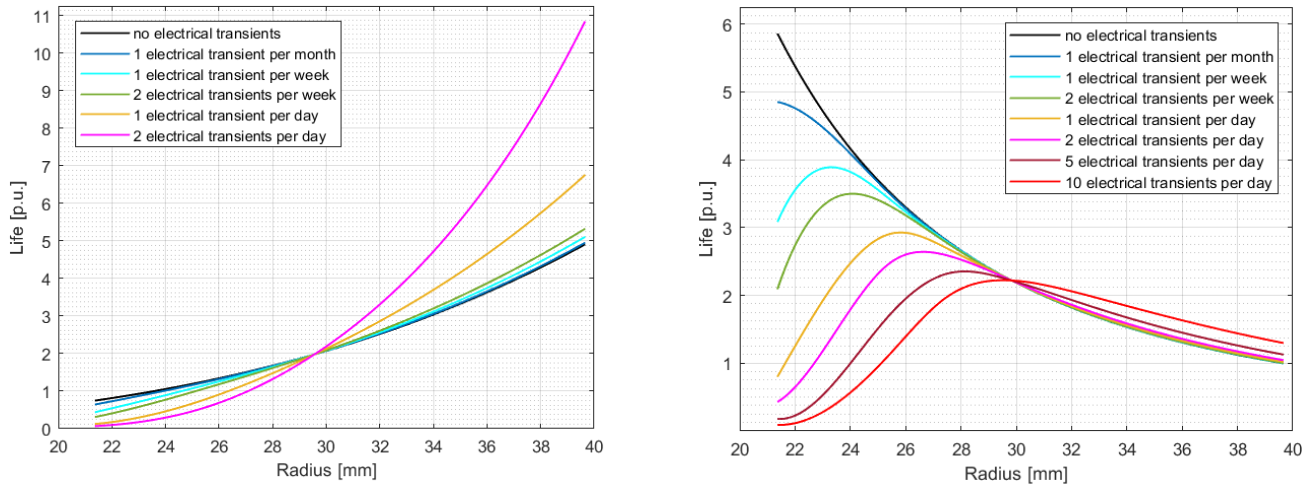

Fig. 5. Life distribution in p.u. (base value is design life L_D) inside the insulation thickness in linear scale for several numbers of electrical transients for a hot reference cable ($r_i = 21.4$, $r_o = 39.7$ mm) and (a) $a = 0.042$ and (b) $a = 0.084$.

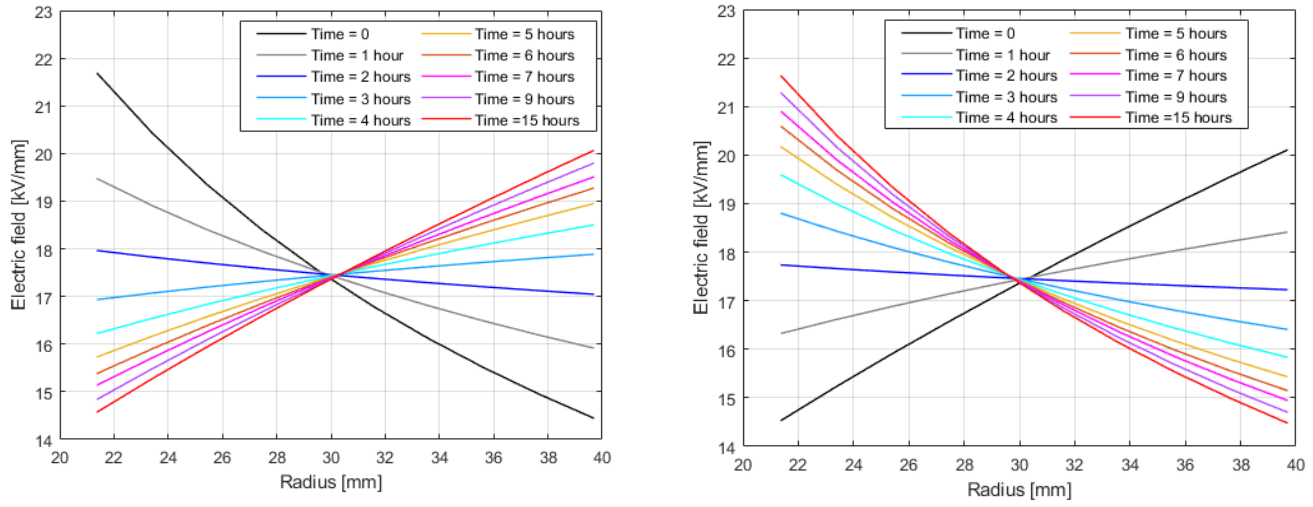

Fig. 6. Electric field during thermal transients (a) T1→ T2 transient and (b) T2→ T1 transient.

IV. Results and Discussion

A. Electrical Transients

Electrical transients, with reference to Table II, are applied on the cable for two values of a (low and medium), for the sake of comparison. Fig. 4 presents the so-called life map which shows the equi-life loci for all feasible designs in (r_i, r_o) coordinates ranging in $(5 \div 50{,}10 \div 80)\, mm$, as fully illustrated in the part 1 of this paper [11]. Fig. 4 shows that the greater the number of electrical transients, the shorter the life. The latter demonstrates the need to enlarge the cable geometries to sustain the design life, which in turn shifts the equi-life loci upward. Comparing Fig. 4(a) to 4(f), a more severe effect of transients on cable life can be noticed when the dielectric is characterized by a low value of a. In the worst case simulated here ($a = a_L$, Fig. 4(a), 4(b), and 4(c)), two polarity reversals per day are enough to increase the cable design thickness by ≈ 10 mm. On the other hand, when $a = a_m$ (Fig. 4(d), 4(e), and 4(f)), insulation thickness increases by ≈ 5 mm for the same number of transients. This is justified by the fact that low values of a will also imply lower values of conductivity, see (5). This will in turn increase the electrical time constant, hence the duration of transient conditions during which the insulation will locally have to withstand enhanced fields (see Fig. 1). For the sake of clarity, the life distribution inside the insulation thickness can also be analysed. In Fig. 5(a) and 5(b), it can be seen how electrical transients have a more detrimental effect on the inner insulation of dielectrics with lower values of a, since in this case the electric field is always maximum near the inner conductor of the cable (see Fig. 1(a)) . For higher values of a, the life distribution pattern can be non-monotone, due to field inversion. In this case, at steady state the outer insulation will be more stressed than the inner insulation, while the opposite occurs during transient conditions (Fig. 1(b)). As a result, when no transients are considered, life is always related to the failure of the outer insulation. Introducing a number of transients, however, will modify life distribution and, from a certain amount (e.g. 1 electrical transient per day), life minimum can shift towards the inner insulation. This is also the reason why Fig. 4(d) and 4(e) seem identical. It can be also noticed in Fig.

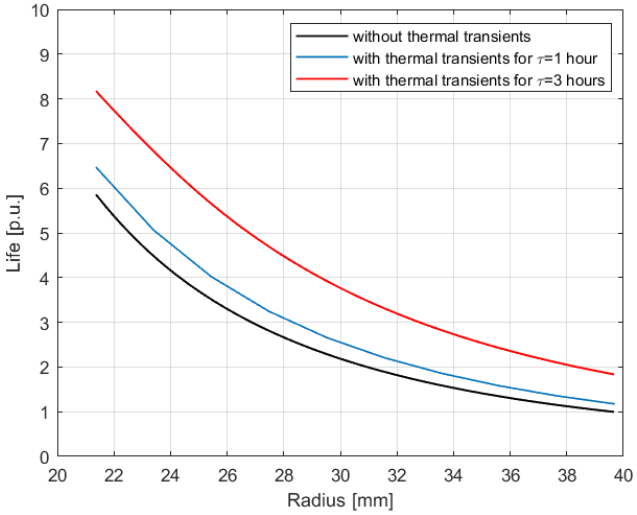

Fig. 7. Total life in p.u. (base value is L_D) during both the thermal transients and the steady state.

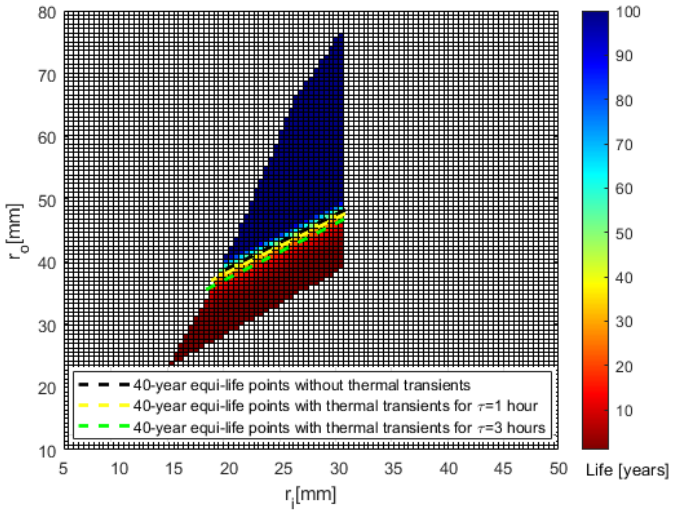

Fig. 8. The effect of thermal transients on the life map.

4 that the increase in the inner insulation radius leads to a significant reduction of the effect of electrical transients on the life (i.e. 40-year life loci are converging). This is caused by the reduction of both steady state and transient electric field inside the insulation thickness.

B. Thermal Transients

Thermal transients are applied on the cable in the form of load cycles, each cycle consists of two transients LT→HT and HT→LT according to Table III, see Fig. 2. Fig. 6 illustrates electric field variation over time for both types of thermal transients. It can be noticed that the electric field distribution is quasi-capacitive in the cold cable, since an isothermal condition is considered at this stage. Hence, conductivity will be almost homogeneous (as only a slight effect of field coefficient b is observed), and field distribution in DC will be practically the same as in AC. Hence, the inner insulation is the most stressed part of the insulation at this stage. On the contrary, in the hot cable, the electric field distribution becomes resistive and the outer insulation is the most stressed point. Results from simulations considering a constant applied voltage $U = U_0$ and thermal transients with different time constants (Fig. 7) show that life minimum is generally found in the outer insulation, since field redistribution due to thermal transients are usually faster than in the cases discussed in section IV–A, hence most of life reduction will be due to steady state conditions. It can also be seen that more thermal transients can relieve electro-thermal stresses during insulation life, extending the amount of time characterized by intermediate field distributions, when a lower maximum value is found in the insulation (Fig. 6). As a result, life in the insulation is increased for longer values of the thermal time constant τ_T (Fig. 7). The effect on life due to exclusively thermal stresses at different values of τ_T can be noticed considering the insulation at $r \approx 30\ mm$, where the electric field is mostly constant during thermal transients (Fig. 6). Considering this point, life increases by 67% due to the sole contribution of an average thermal stress reduction HT→LT. Fig. 8 shows the effect of temperature transients on life map, with different time constants. Due to the positive effects of longer thermal time constants, smaller design geometries of the cable are allowed for the same life. In other words, equi-life loci are shifted toward smaller insulation thicknesses. Life minimum (hence cable life) in the reported case is always found in the outer insulation, but it should be mentioned that this is not the case when no field inversion is present at steady state (i.e. materials with lower values of the temperature coefficient a, as can also be seen in the Section IV–C).

C. Electro-thermal Transients

Fig. 9 illustrates the combined effect of electrical and thermal transients on the total life of cable. One thermal and one electrical transients per day are applied in a non-simultaneous way on the reference cable, considering $a = 0.042$ (Fig. 9(a)) and $a = 0.084$ (Fig. 9(b)). Results show, in the red curve, the combined effect of electrical and thermal transients on the life of different points distributed within the insulation. The case represented in Fig. 9(a) shows that the combination of electrical and thermal transients does not induce a substantial difference on cable life, since its minimum is always found near the inner insulation, and the effect of electro-thermal transients are similar to that of the sole electrical transients. This can be explained reminding that most of life loss of the inner insulation is occurring during transients, when local field is increased. A closer look reveals a mild increase of life minimum in the case of electrothermal transients, due to slightly lower average temperatures experienced by the insulation during life (which is the reason behind the life increase observed with purely thermal transients). Life near the outer insulation is, on the other hand, higher in the presence of combined transients since it will benefit from both the local electric field reduction due to the electrical part of transients, and an average lower temperature due to the thermal part of transients. As can be noticed, life distribution after combined transients is monotonically increasing since both thermal and electrical stresses are generally decreasing with the considered radius. On the other hand, the case of Fig. 9(b) shows that life distribution following

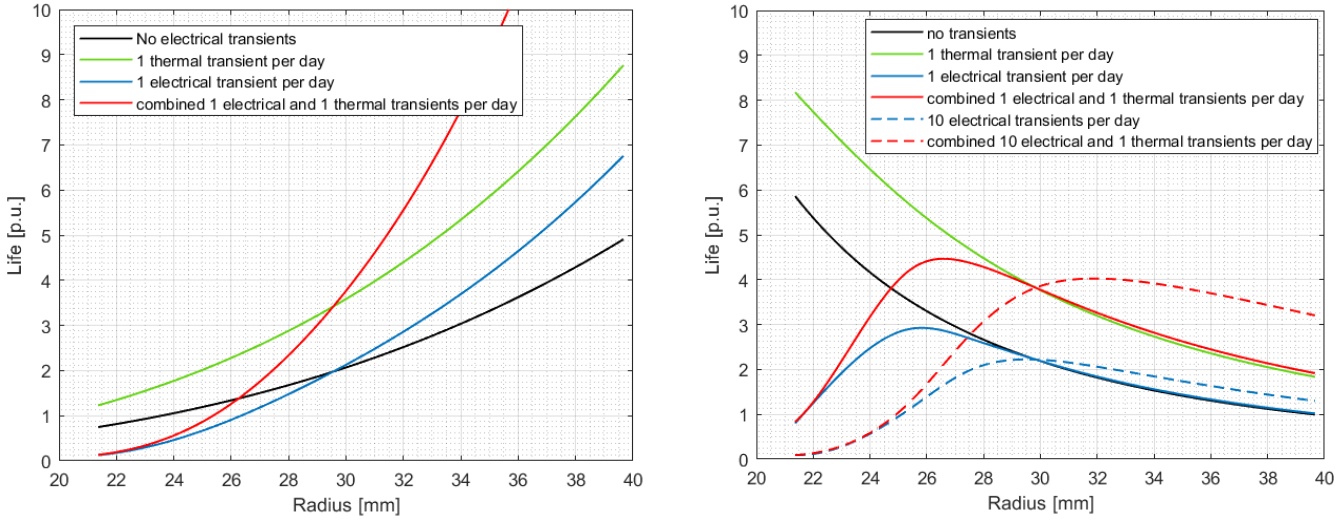

Fig. 9. Total life of a hot reference cable with combined non-simultaneous electrical and thermal transients for (a) $a = 0.042$ and (b) $a = 0.084$.

combined transients can also be non-monotone. That is the case when the average electric stress is distributed in a non-monotone manner (as mentioned in Section IV–A), while thermal stress is monotonous. As a result, life of insulation near the inner conductor is, as before, similar for both the electrical and combined transients, for the same reason discussed above. On the other hand, results closer to the outer regions are mostly similar to life in the case of thermal transients, since the influence of electrical transients is negligeable (notice that in Fig. 9(b) life with and without electrical transients are practically the same in those regions). To further emphasize the role played by electrical transients, the quite severe – and far from reality, see above - case where 10 electrical transients per day take place throughout the cable life (combined or not with thermal transients) has also been considered in Fig. 9(b). In this case, the cable life at inner insulation is dramatically reduced with respect to design life. It must be noticed that this study shows the effect of transients on only electrothermal life of cable. Other types of stress are out of the scope of this paper. In fact, thermal load cycles cause consecutive heating (expansion) and cooling (contraction) of the cable components, resulting in radial and circumferential stresses in the insulation [30].

V. Conclusion

This paper, which is the second part of two companion papers, investigates the effect of polarity reversal events as electrical transients in addition to thermal transients on the electrothermal life map of HVDC cables and their influence on the cable geometries. The results show that the field enhancement in the inner insulation due to electrical transients leads to life reduction of the cable. This shifts the equi-life loci toward greater cable radii. A material characterized by lower temperature coefficient of electrical conductivity, a, enhances this detrimental effect due to an increased electrical time constant of the dielectric, requiring longer time to reach stability (hence an extension of high local stress conditions). Conversely, thermal transients relieve the average thermal stress applied on the insulation, increasing insulation life and extending feasibility towards smaller cables. The effects of the combination of those transients are dependent on two separate contributions: one negative, from the electrical part of the transient, and one positive, from the thermal part of the transient. The resulting cable life is generally similar to the one found after an equal amount of purely electrical transients, with minor benefits from temporary temperature reduction.

References

[1] G. Mazzanti and M. Marzinotto, *Extruded Cables for High Voltage Direct Current Transmission: Advance in Research and Development*, Power Engineering Series, Wiley-IEEE Press, 2013.

[2] G. Mazzanti, “Issues and challenges for HVDC extruded cable systems,” Energies (MDPI), vol. 14, no 15, pp. 1-34, 2021.

[3] 50Hertz Transmission GmbH; Amprion GmbH; Tennet TSO GmbH; TransentBw GmbH. Grid Development Plan. (GDP) 2030, 2nd Draft; Technical Report; German TSOs: Berlin, Germany, 2019.

[4] Wikipedia. Western HVDC Link. Available online: https://en.wikipedia.org/wiki/Western_HVDC_Link#cite_notewesternhvdclink-mc-4 (accessed on Semptember 9th 2021).

[5] M. Jeroense, P. Bergelin, T. Quist, A. Abbasi, H. Rapp, and L. Wang, “Fully qualified 640 kV underground extruded DC cable system,” paper B1-309, 2018 CIGRE Session.

[6] M. Albertini, S. Franchi Bononi, S. Giannini, G. Mazzanti, N. Guerrini, “Testing challenges in the development of innovative extruded insulation for HVDC cables”, IEEE Electr. Insul. Mag. Vol. 37, No. 6, Nov. Dec. 2021.

[7] G. C. Montanari and P. Seri, "HVDC and UHVDC polymeric cables: Feasibility and material development," IEEE Electr. Insul. Mag., vol. 35, no. 5, pp. 28-35, Sept.-Oct. 2019.

[8] G. Mazzanti and B. Diban, "The Effects of Transient Overvoltages on the Reliability of HVDC Extruded Cables. Part 1: Long Temporary Overvoltages," in IEEE Trans. Power Deliv. , vol. 36, no. 6, pp. 3784-3794, Dec. 2021.

[9] G. Mazzanti and B. Diban, "The Effects of Transient Overvoltages on the Reliability of HVDC Extruded Cables. Part 2: Superimposed Switching Impulses," in IEEE Trans. Power Deliv., vol. 36, no. 6, pp. 3795-3804, Dec. 2021.

[10] A. Battaglia, M. Marzinotto and G. Mazzanti, "A Deeper Insight in Predicting the Effect of Voltage Polarity Reversal on HVDC Cables," 2019 IEEE Conf. Electr. Insul. Dielectr. Phenom. (CEIDP), 2019, pp. 442-445

[11] B. Diban, G. Mazzanti, P. Seri, "Life-based Geometric Design of HVDC cables. Part 1: Parametric Analysis," IEEE Trans. Dielectr. Electr. Insul., vol. 29, no. 3, pp. 973-980, June 2022.

[12] C. K. Eoll, "Theory of stress distribution in insulation of high voltage d.c. cables. Part I," IEEE Trans. Electr. Insul., vol. EI-10, no. 1, pp. 27–35, 1975.

[13] B. Diban, and G. Mazzanti, "The effect of temperature and stress coefficients of electrical conductivity on the life of HVDC extruded cable insulation subjected to type test conditions," IEEE Trans. Dielectr. Electr. Insul., vol. 27, no. 4, pp. 1295-1302, Aug. 2020.

[14] H. Naderiallaf, P. Seri and G. C. Montanari, "Designing a HVDC Insulation System to Endure Electrical and Thermal Stresses Under Operation. Part I: Partial Discharge Magnitude and Repetition Rate During Transients and in DC Steady State," in IEEE Access, vol. 9, pp. 35730-35739, 2021.

[15] B. Diban, G. Mazzanti, M. Marzinotto, and A. Battaglia, "Calculation of Electric Field Profile within HVDC Cable Insulation in the Presence of Voltage Polarity Reversals," presented in IEEE Int. Conf. Dielectr. ICD, Palermo, Italy, July. 2022.

[16] M. J. P. Jeroense and P. H. F. Morshuis, "Electric fields in HVDC paper insulated cables," IEEE Trans. Dielectr. Electr. Insul., vol. 5, no. 2, pp. 225-236, April 1998.

[17] IEC 60853-2, Calculation of the Cyclic and Emergency Current Rating of Cables, Part 2: Cyclic Rating of Cables Greater Than 18/30 (36) kV and Emergency Ratings for Cables of All Voltages, Ed. 1.0, Jan. 1989 + Amd. 2008.

[18] Y. Zhang, X. Zhou, H. Niu, X. Wang, Y. Tang, J. Zhao, and Yo. Fan, "Theoretical calculation and experimental research on thermal time constant of single-core cables," High Voltage Engineering, vol. 35, no. 11, pp. 2801-2806, Nov. 2009.

[19] I. Garniwa and A. Burhani, ''Thermal incremental and time constant analysis on 20 kv XLPE cable with current vary,'' in Proc. IEEE 8th Int. Conf. Properties Appl. Dielectr. Mater., Jun. 2006, pp. 566–569.

[20] A. Henke, and S. Frei. "Transient temperature calculation in a single cable using an analytic approach.," Int. J. Heat Fluid Flow (JFFHMT) , vol. 7, no. 1, pp. 58-65, 2020.

[21] H. Naderiallaf, P. Seri and G. C. Montanari, "Investigating Conditions for an Unexpected Additional Source of Partial Discharges in DC Cables: Load Power Variations," in IEEE Trans. Power Del., vol. 36, no. 5, pp. 3082-3090, Oct. 2021.

[22] G. Mazzanti, "The effects of seasonal factors on life and reliability of high voltage AC cables subjected to load cycles," IEEE Trans. Power Deliv., vol. 35, no. 4, pp. 2080-2088, Aug. 2020,

[23] G. Mazzanti, "Life estimation of HVDC cables under the time-varying electrothermal stress associated with load cycles", IEEE Trans. Power Del., vol. 30, no. 2, pp. 931 – 939, Apr. 2015.

[24] G. Mazzanti, "Including the Calculation of Transient Electric Field in the Life Estimation of HVDC Cables Subjected to Load Cycles," IEEE Electr. Insul. Mag., Vol. 34, No. 3, pp. 27-37, 2018

[25] M. A. Miner, "Cumulative damage in fatigue," J. Appl. Mechan., pp.A159–A163, Sep. 1945.

[26] R. N. Hampton, "Some of the considerations for materials operating under high-voltage, direct-current stresses," IEEE Electr. Insul. Mag., vol. 24, no. 1, pp. 5–13, 2008.

[27] Recommendations to improve HVDC cable systems reliability. Available online: https://europacable.eu/wp-content/uploads/2021/01/Joint-paper-HVDC-Cable-Reliability-ENTSO-E-Europacable_FINAL_13.06.2019_.pdf

[28] R. Huang, "Dynamic Rating for Improved Operational Performance," PhD dissertation, University of Southampton, 2015.

[29] P. Chatzipanagiotou, V. Chatziathanasiou, G.D. Mey, B. Wiecek, "Influence of soil humidity on the thermal impedance, time constant and structure function of underground cables: a laboratory experiment," Appl. Therm. Eng., vol. 113, pp. 1444-1451, 2017.

[30] N. Guerrini, G. Mazzanti, B. Diban, I. Troia, "Validation of Mechanical Features of HPTE Insulation for EHV DC Land Cable Systems," 2021 Conf. Electr. Insul. Dielectr. Phenom. (CEIDP), virtual conference, 2021, pp. 208-210.

Bassel Diban (Member, IEEE) received the bachelor's degree in electrical power engineering from Damascus University, Damascus, Syria (2014), then he joined the Syrian TSO for two years, and later received the master's degree in electrical energy engineering from the University of Bologna, Bologna, Italy (2019), where he is currently pursuing the Ph.D. degree.

His research interests are life modeling, reliability, diagnostics of HV insulation, and HVDC cable systems.

Mr. Diban is a member of the IEEE DEIS Technical Committee (TC) on "High Voltage Direct-Current (HVDC) cable systems".

Giovanni Mazzanti (Fellow, IEEE) is currently an Associate Professor of HV Engineering and Power Quality at the University of Bologna, Bologna, Italy. He is Consultant to TERNA (the Italian TSO), Rome, Italy. His research interests are reliability and diagnostics of HV insulation, power quality, renewables, and human exposure to EMF. He has authored or coauthored more than 300 published papers, and book *Extruded Cables for HVDC Transmission: Advances in Research and Development*, (Wiley-IEEE Press, 2013).

Mr. Mazzanti is a member of IEEE PES and DEIS, IEEE DEIS Technical Committee (TC) on "Smart grids," CIGRÉ, CIGRÉ Joint Working Group B4/B1/C4.73 on "Surge and extended overvoltage testing of high voltage direct-current (HVDC) cable systems." He is the Chair of the IEEE DEIS TC on "HVDC cable systems."

Paolo Seri (Member, IEEE) was born in Macerata, Italy, in June 4, 1986. He received the master's degree in energy engineering and the Ph.D. degree in electrical engineering from the University of Bologna, Bologna, Italy, in 2012 and 2016, respectively.

In 2017, he was with the Laboratory of Innovative Materials for Electrical Systems (LIMES), University of Bologna, as a Research Fellow, where he is currently working on the topics of high voltage direct-current (HVDC) cables design, partial discharge detection and modeling, and characterization of dielectric materials. He is also a Researcher with the Department of Electrical, Electronic and Information Engineering (DEI), University of Bologna.